MODELING OF THE DYNAMIC RESPONSE OF A FRANCIS TURBINE

Paolo PENNACCHI, Steven CHATTERTON*, Andrea VANIA

Politecnico di Milano, Department of Mechanical Engineering - Via G. La Masa, 1 - 20156 - Milano, Italy.

KEYWORDS: hydroelectric power plant model, pressure waves, Francis turbine.

ABSTRACT

The paper presents a detailed numerical model of the dynamic behaviour of a Francis turbine installed in a hydroelectric plant. The model considers in detail the Francis turbine with all the electromechanical subsystems, such as the main speed governor, the controller and the servo actuator of the turbine distributor, and the electrical generator. In particular, it reproduces the effects of pipeline elasticity in the penstock, the water inertia and the water compressibility on the turbine behaviour. The dynamics of the surge tank on low frequency pressure waves is also modeled together with the main governor speed loop and the position controllers of the distributor actuator and of the hydraulic electrovalve. Model validation has been made by means of experimental data of a 75 MW - 470 m hydraulic head - Francis turbine acquired during some starting tests after a partial revamping, which also involved the control system of the distributor.

NOMENCLATURE

$\Delta\bar{\omega}$	Deviation of rotational speed in p.u.
$\Delta\bar{G}$	Deviation of gate opening in p.u.
$\Delta\bar{H}_t$	Deviation of turbine hydraulic head in p.u.
$\Delta\bar{P}_m$	Deviation of mechanical power in p.u.
$\Delta\bar{U}_t$	Deviation of water velocity in p.u.
ϕ_p	Friction energy term of the penstock
ϕ_c	Friction coefficient of the tunnel

* Corresponding author: email: steven.chatterton@polimi.it, ph: +39 02 23998442, fax: +39 02 23998492

ρ	Volumetric mass of water
τ_p	Time constant of the servovalve
ω_0	Rotational speed in operating condition
A_p	Penstock area
b_p, b_t, T_x, T_d, T_3	Gains and time constants of the speed controller in operating mode
C_I	Proportional gain of the gate opening controller
C_x	Flow gain of the servovalve
c_p	Wave velocity in the penstock
D	Damping factor
D_{ck}	Diameter of the *k*-th tunnel (*k* = 1,2)
D_p	Penstock diameter
$\overline{e}_\omega$	Rotational speed error in p.u.
E	Young's modulus of elasticity of pipe material
f	Thickness of pipe wall
g	Gravitational acceleration
$G_0, \overline{G}_0$	Gate opening reference signal and p.u. form
G	Actual gate opening
$H, (H_0)$	Hydraulic head at gate (in operating condition)
I_0	Current command input of the servovalve
J	Generator inertia
k_1	Gain constant of the servovalve
k_b	Hydraulic cylinder net area constant
k_f	Friction coefficient of the penstock
k_p, k_i	Gains of the PI speed controller in starting mode
K	Bulk modulus of water compression
K_i	Inertia constant
K_u, K_p	Velocity and power constants
L_{ck}	Length of the *k*-th tunnel (*k* = 1,2)
L_p	Penstock length
$P_m, (P_{m0})$	Turbine mechanical power (in operating condition)
p_t	Water pressure at gate
q_{oil}	Oil flow in the hydraulic cylinder
Q_0	Turbine water flow in operating condition
T_a	Mechanical starting time
$\overline{T}_e$	Electrical load torque in p.u.
T_{ep}	Elastic time of the penstock
$\overline{T}_m$	Mechanical torque of the turbine in p.u.
T_s	Time constant of the surge tank
T_{Wc}	Starting time of the tunnel

T_{Wp}	Water starting time of the penstock
$U,(U_0)$	Water velocity (in operating condition)
x	Pilot valve spool position
Z_p	Penstock normalized hydraulic surge impedance
Z_{p0}	Hydraulic surge impedance of the penstock

1 INTRODUCTION

The accurate dynamic model of turbine units in hydroelectric plants assumes great importance in case of renewal of turbine components, such as the control and the actuator systems, or in case of periodic and required inspection of the emergency systems. In this sense, a model of the entire system prevents dangerous conditions during the tuning of the control system and provides a reference response for inspections.

This kind of model could be also used during design phases, for penstock dimensioning, for the overspeed estimation and for the analysis of new control strategies of the speed governor.

The first studies about power system of hydro turbines date back to the early 70s, when a task force on overall plant response was established in order to consider the effects of power plants on power system stability and to provide recommendations regarding problems not already investigated. The outcome of this effort has been a first simple model consisting in transfer functions of the speed governing and the hydro turbines systems [1].

However, these early models were inadequate to study large variations of power output and frequency. For instance, they were not reliable in the very low frequency range, as they did not account for the water mass oscillations between the surge tank and the reservoir, and at high frequency [2], as they did not reproduce water hammer effects.

To solve these limitations, some improvements of both turbine and speed control models were made by the Working Group on Prime Mover and Energy Supply Models for System Dynamic Performances Studies [3].

In this paper, the authors propose a detailed and complete numerical model of the dynamic behaviour of a Francis turbine of a hydroelectric plant. The model considers in detail the Francis turbine with all the electromechanical subsystems, such as the main

speed governor, the controller and the servo actuator of the turbine distributor, and the electrical generator. In particular it reproduces the effects of pipeline elasticity in the penstock, the water inertia and the water compressibility on the turbine behaviour. Among the different possible approaches for the pressure wave modelling, the transfer function method is employed in this paper, allowing testing different closing manoeuvres of turbine distributor performed by the control system. The dynamics of the surge tank and of the reservoir on low frequency pressure waves are also modelled together with the main governor speed loop and the position controllers of the distributor actuator and of the hydraulic electrovalve.

The proposed model has been successfully validated by means of experimental data of a 75 MW - 470 m hydraulic head - Francis turbine of a hydroelectric plant, acquired during some starting tests after a partial revamping, which also involved the control system of the distributor.

2 PLANT DESCRIPTION

The Francis turbine unit here considered belongs to a complex hydroelectric basin, in southern Italy, consisting of three hydroelectric plants, placed in series.

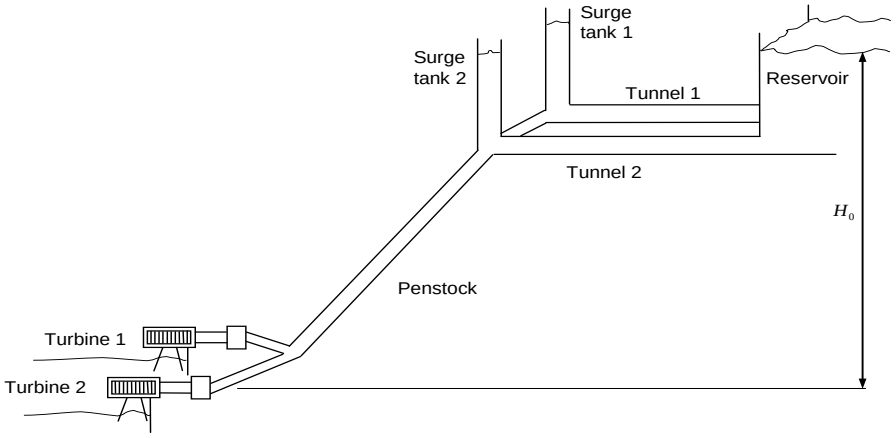

Figure 1 Hydraulic scheme of the first plant.

The first hydroelectric plant, shown in Figure 1 is constituted of two 75 MW Francis turbines working at 600 rpm, with a hydraulic head of about 470 m. The two vertical-axis turbines are supplied by means of a single steel penstock from two interconnected surge tanks, each of them connected to a lake reservoir by two rocky tunnels.

The discharged water of the first plant supplies a second reservoir used by the second plant and so on also for the last plant. The main data of the plant are reported in Table 1.

Table 1. Data of the hydroelectric central

L_{c1}	Tunnel 1 length	4190 m
D_{c1}	Tunnel 1 diameter	2.5 m
L_{c2}	Tunnel 2 length	4111 m
D_{c2}	Tunnel 2 diameter	3.2 m
L_p	Penstock length	1220 m
D_p	Penstock diameter	3 m
f	Thickness of pipe wall	0.020 m
Q_{0t}	Penstock overall rated flow	35 m^3/s
H_0	Hydraulic head	440.37-474.43 m
J_{PD^2}	Generator inertia PD^2	600 10^3 kgm^2
Q_0	Single turbine rated flow	17-18 m^3/s
P_r	Single turbine electric power	66.3-75.2 MW
ω_0	Rated speed	600 rpm

A spherical valve, moved by a hydraulic actuator, is placed at the end of the penstock as shown in Figure 2. This valve operates only during starting, emergency phases and stopping.

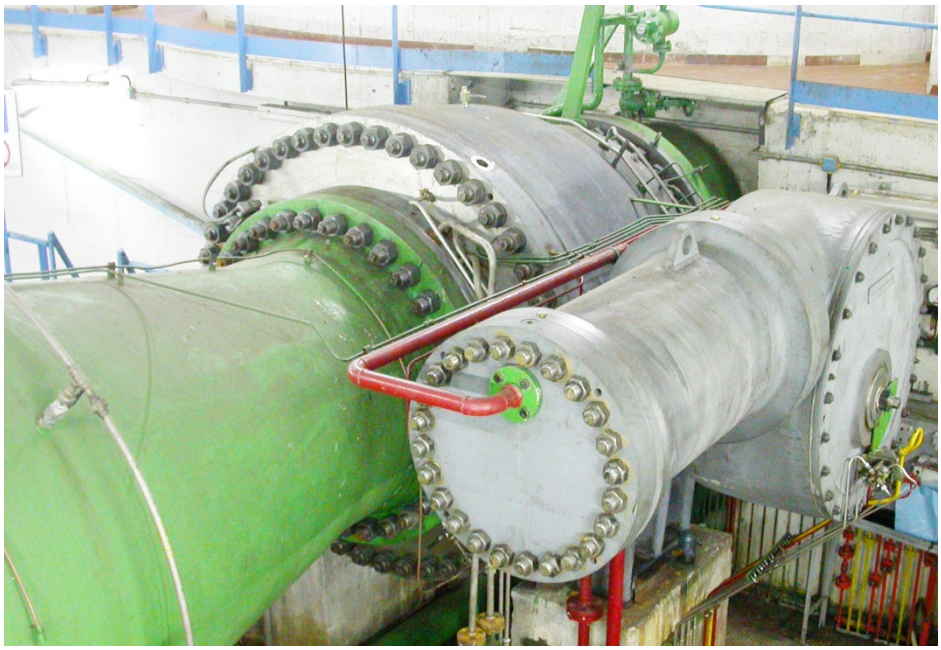

Figure 2 Spherical valve at the end of the penstock.

The generator is an 80 MVA-10 kV three-phase synchronous machine running at 600 rpm. The upper part of the exciter system of the generator is shown in Figure 3.

Figure 3 Upper part of the generator exciter system.

The considered plant is an *early restoration plant*, namely one of the hydroelectric plants able to restore a power system after a blackout through preestablished path called *restoration lines*. The turbines of these stations are equipped with special speed governors for that purpose.

The rotational speed of the Francis turbine is controlled by modifying the water flow in the turbine, by means of the distributor system. The distributor consists of steerable blades placed before the inlet of the runner and interconnected together by means of a ring. The rotation of the blades, performed by the ring, modifies the section areas of the guide vanes that is the flow in the turbine. The rotation of the ring is realized by means of a hydraulic cylinder (servomotor) as shown in Figure 4.

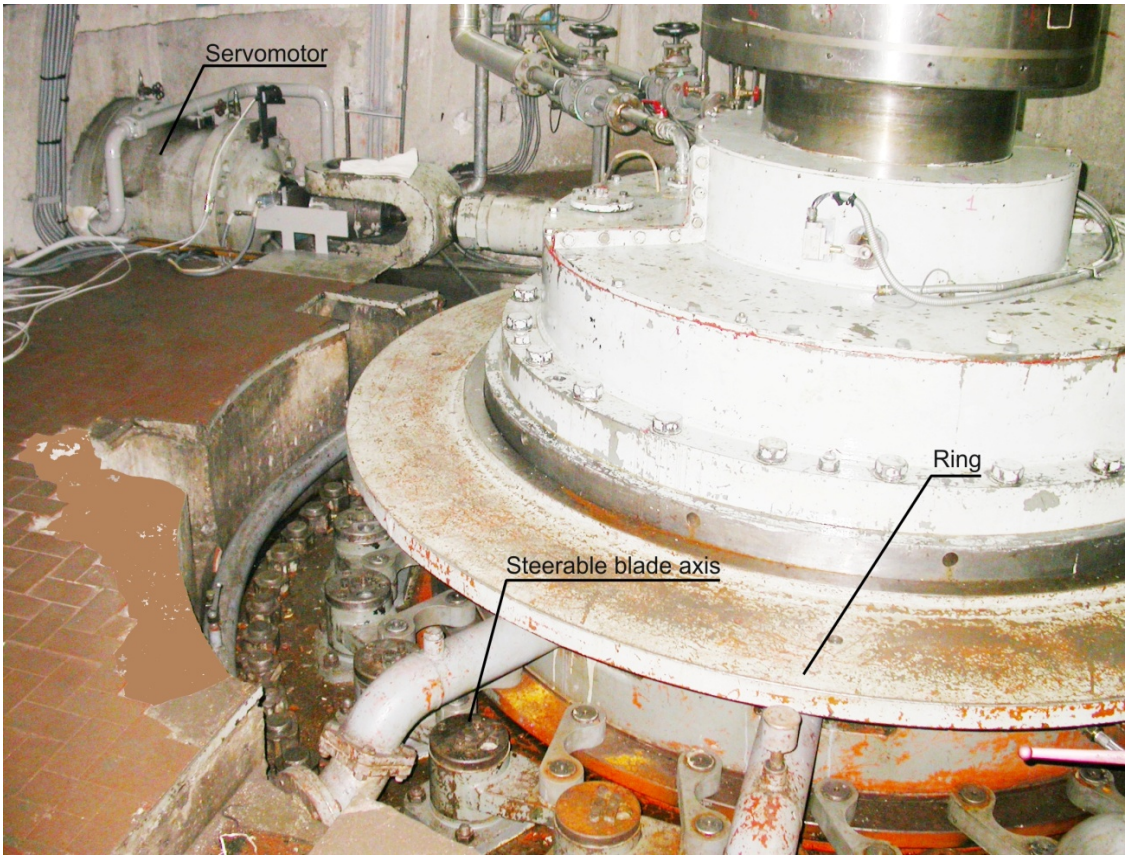

Figure 4 Distributor system of the Francis turbine.

As said before, the experimental tests, described in the next section, were performed after the renewal of the control system unit (Figure 5) of the servomotor.

Figure 5 Hydraulic control unit of the servomotor.

3 MODEL OF THE SYSTEM

The functional block diagram of the hydroelectric plant is shown in Figure 6, where only a single turbine unit is considered [4]. It mainly consists of the speed changer, the speed regulator, the distributor, the turbine and the generator.

For the safety of the electric network, the frequency should remain almost constant. This is ensured by keeping constant the speed of the synchronous generator.

The speed changer (external central control) gives the reference speed signal, depending on the power network requirements, since the frequency depends on the active power balance of the network.

The rotational speed of the turbine is fed back and modified by the speed governor acting on the turbine distributor (gate) by means of the hydraulic servomotor. The turbine mechanical power is essentially a function of gate position.

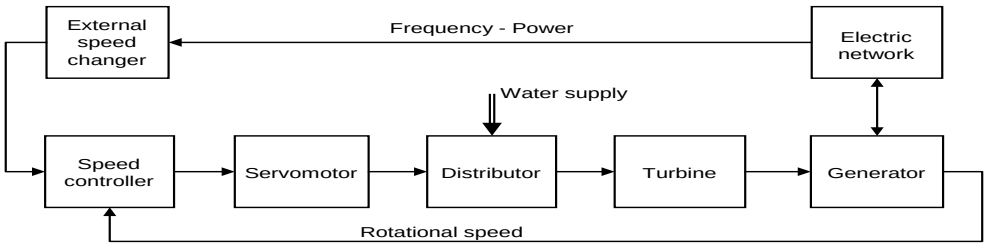

Figure 6 Functional block diagram of the overall system.

The details of each submodel shown in Figure 6 are analysed in the following sections.

3.1 Speed controller model

For a stable division of the load between two or more generating unit operating in parallel, the speed governors are generally provided with a permanent *droop characteristics* so that the speed drops when the load decrease [5],[6]. The simple presence of the droop characteristics on the regulator causes a steady-state frequency error that could be reduced operating compensation in the regulator scheme. A large transient (temporary) droop [7] with a long resetting time is also included in the regulator transfer function by means of a suitable transfer function in order to improve the stability of the control.

The actual speed regulator implemented consist of two operating modes: the *starting mode* for run-ups from standstill to steady-state without load and the *operating mode* for nominal operating condition at rated speed and with an active load. The switching from the two operating mode is done in a bumpless way. The starting mode consists of a simple PI regulator including an integral anti windup in the implemented algorithm:

$$F_{starting}(s) = \frac{\bar{G}_0}{\bar{e}_\omega} = k_p + \frac{k_i}{s} \tag{1}$$

where $\bar{G}_0$ is the normalized gate opening reference signal and $\bar{e}_\omega$ is the error of the normalized rotational speed.

The operating mode is represented by a two-pole and two-zero transfer function:

$$F_{operating}(s)=\frac{\bar{G}_0}{\bar{e}_\omega}=\frac{1}{b_p}\frac{\left(\frac{T_x}{b_t}s+1\right)}{\left(\frac{T_x}{b_p}s+1\right)}\frac{(T_d s+1)}{(T_3 s+1)} \quad (2)$$

The final control scheme including the speed compensations is shown in Figure 7, where two compensation terms are added to the reference signal of the gate opening. The steady-state compensation allows reducing the steady-state rotational speed error due to the droop characteristics, whereas the variable compensation is a feed-forward term depending on the electrical load.

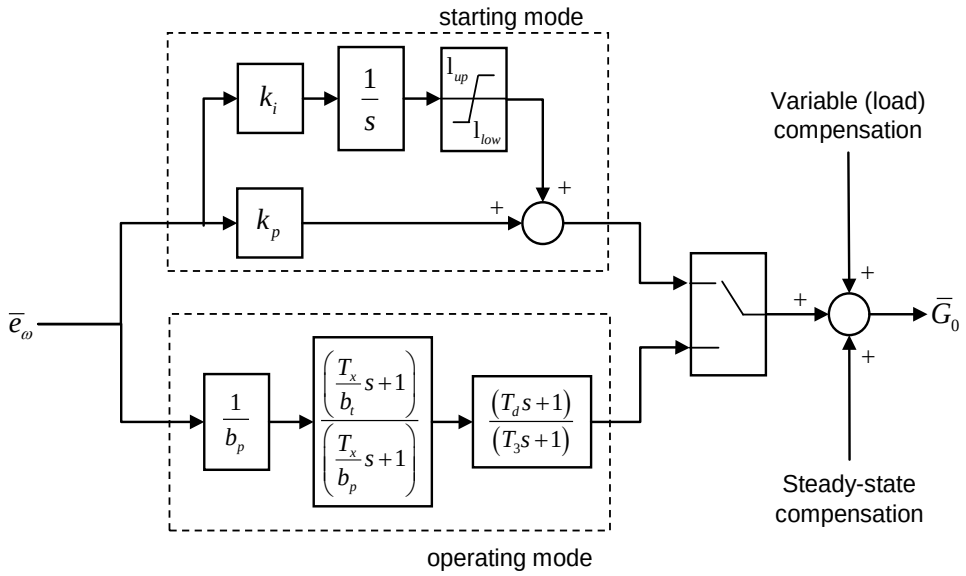

Figure 7 Speed controller block diagram.

3.2 Servomotor system model

The output of the speed regulator is proportional to the reference gate opening signal. The gate opening is actuated by the hydraulic cylinder (servomotor) that rotates the ring of the distributor allowing flow changes. The servomotor is position controlled, by acting on the cylinder oil flow by an electrovalve that receives as input the reference gate opening signal. The speed of the cylinder stem is proportional to the supplied oil flow in the cylinder chamber. Thus, the simplest first order transfer function of the cylinder that relates the actual gate opening G to the oil flow q_{oil} could be written as:

$$F_c(s) = \frac{G(s)}{q_{oil}(s)} = k_b \frac{1}{s} \tag{3}$$

where k_b is a suitable constant representing the cylinder net area and the linear assumed relationship between the cylinder position and the gate opening.

The oil flow could be also assumed proportional to the position x of the pilot valve spool:

$$q_{oil} = C_x x \tag{4}$$

where C_x is the flow gain of the electrovalve.

A position control is also actuated to the spool of the servovalve. The behaviour of the servovalve could be described by a first order transfer function relating the spool position x to the current input I_0:

$$F_{I-x}(s) = \frac{I_0(s)}{x(s)} = \frac{k_1}{\tau_p s + 1} \tag{5}$$

where τ_p is the time constant of the servovalve and k_1 a suitable constant.

A simple proportional position control of the gate opening is implemented in the plant controller:

$$I_0(s) = C_I(G_0 - G) \tag{6}$$

The block diagram of the gate opening control including the servovalve and the servomotor transfer functions is shown in Figure 8.

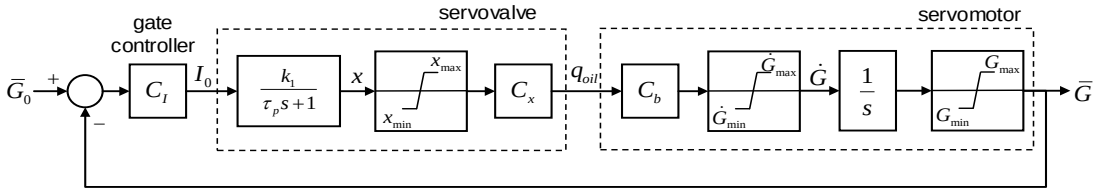

Figure 8 Block diagram of the gate position control loop.

The nonlinearities due to the limits on the position of the servovalve and to the limits on the speed and position of the gate are also reported in Figure 8.

3.3 Turbine model

The dynamic behaviour of a hydraulic turbine operating at full load is widely described by a transfer function that relates the deviation of the output mechanical power to the deviation of gate opening [5],[8].

The turbine-distributor system is modelled as a valve, where the velocity U of the water at gate is given by:

$$U = K_u G\sqrt{H} \tag{7}$$

The turbine mechanical power is proportional to the product of pressure and flow:

$$P_m = K_p HU \tag{8}$$

where K_u and K_p are proportional constants, G is the gate (distributor) opening, and H is the hydraulic head at the gate.

By linearizing and considering both small displacements about the operating point and p.u. expressions, it follows:

$$\frac{\Delta\overline{P_m}(s)}{\Delta\overline{G}(s)} = \frac{1+\dfrac{1}{F(s)}}{1-\dfrac{1}{2}\dfrac{1}{F(s)}} \tag{9}$$

where $\Delta\overline{P}_m = \Delta P_m / P_{m,0}$ is the p.u. small deviation of the hydraulic (or mechanical) power (corresponding to the p.u. mechanical torque), $\Delta\overline{G}$ is the p.u. small deviation of the gate opening and $F(s) = \Delta\overline{U}_t(s)/\Delta\overline{H}_t(s)$ is the transfer function that relates the normalized flow (corresponding to the p.u. water speed) to the normalized hydraulic head deviation at gate.

3.3.1 Classical model

The classical model of the ideal turbine is obtained considering [1],[9]:

$$\frac{1}{F(s)} = -T_{Wp}s \tag{10}$$

where T_{Wp} is the *water starting time* (or *water time constant*) of the penstock at rated load, that depends on the load conditions. The starting time represents the time required

for a total head H_0 to accelerate the water in the penstock of length L_p from standstill to the velocity U_0:

$$T_{Wp} = \frac{L_p U_0}{g H_0} \tag{11}$$

Different values of T_{Wp} are used in the model depending on the load condition: $T_{Wp} = 0.65\text{s}$ for full load condition ($Q_{0,\,full} = 17.5\,\text{m}^3/\text{s}$), whereas $T_{Wp} = 0.065\text{s}$ for the idling condition ($Q_{0,idling} = 1.75\,\text{m}^3/\text{s}$).

Equations (9) and (10) describe the behaviour of a simple ideal linear model of hydraulic turbine for small deviations from steady-state operating point, considering negligible hydraulic resistance, incompressible water and inelastic penstock pipe.

This model is only a medium-low frequency approximation, with relevant errors in the high frequency range, because it does not include the water hammer phenomenon. The model is not also entirely adequate in the very-low-frequency range, as it does not account for the water-mass oscillations in the tunnel (considered as inelastic) that connects the surge tank and the reservoir [9].

3.3.2 Detailed model

The effects of the travelling waves owing to the elasticity of penstock steel and of the water compressibility could be considered by means of the method of characteristics [10],[11] or by means of a transfer function approach. The first method requires the integration of partial differential equations by means of finite difference method and allows the time evaluation of the hydraulic head and speed in several point of the penstock. Instead, the transfer function approach allows only the evaluation of the same quantities at the turbine level [2].

Considering the presence of the surge tank, the overall and detailed transfer function to be used in eq. (9) becomes [5]:

$$F(s) = \frac{\Delta \bar{U}_t}{\Delta \bar{H}_t} = -\frac{1 + \dfrac{F_1(s)}{Z_p}\tanh\left(T_{ep} s\right)}{\phi_p + F_1(s) + Z_p \tanh\left(T_{ep} s\right)} \tag{12}$$

- $F_1(s)$ is the transfer function that describes the tunnel and surge tank interaction:

$$F_1(s) = -\frac{\Delta \bar{H}_r}{\Delta \bar{U}_p} = \frac{\phi_c + sT_{Wc}}{1 + sT_s\phi_c + s^2 T_{Wc}T_s} \tag{13}$$

- T_{Wc} is the starting time of the tunnel, T_s the time constant of the surge tank and ϕ_c the friction coefficient of the tunnel;
- T_{ep} is the elastic time of the penstock of length L_p, diameter D_p and area $A_p = \pi {D_p}^2 / 4$:

$$T_{ep} = \frac{L_p}{c_p} \tag{14}$$

- c_p is the wave velocity in the penstock given by:

$$c_p = \sqrt{\frac{g}{\alpha_p}} \tag{15}$$

- α_p considers the water compressibility and the pipe elasticity:

$$\alpha_p = \rho g \left(\frac{1}{K} + \frac{D_p}{Ef} \right) \tag{16}$$

- K is the bulk modulus of water compression, E the Young's modulus of elasticity of pipe material and f the thickness of pipe wall;
- Z_p is the normalized value of the hydraulic surge impedance of the penstock Z_{p0} given by:

$$Z_p = Z_{p0} \left(\frac{Q_0}{H_0} \right) \tag{17}$$

- Z_{p0} is the hydraulic surge impedance of the penstock:

$$Z_{p0} = \frac{c_p}{Ag} \tag{18}$$

- ϕ_p represents the friction energy term of the penstock:

$$\phi_p = 2k_f |U_0| \tag{19}$$

The term $\tanh(T_{ep}s)$ in eq. (12) could be written as:

$$\tanh\left(T_{ep}s\right)=\frac{1-e^{-2T_{ep}s}}{1+e^{-2T_{ep}s}}=\frac{sT_e\prod_{n=1}^{\infty}\left[1+\left(\frac{sT_{ep}}{n\pi}\right)^2\right]}{\prod_{n=1}^{\infty}\left[1+\left(\frac{2sT_{ep}}{(2n-1)\pi}\right)^2\right]} \tag{20}$$

The elastic time is related to the time constant by:

$$T_{Wp}=Z_pT_{ep} \tag{21}$$

The pressure at gate could be easily evaluated by:

$$p_t=\left(\Delta\bar{H}_t+1\right)H_0 \tag{22}$$

where $\Delta\bar{H}_t$, depending on the gate opening, could be evaluated by the following transfer function:

$$F_p\left(s\right)=\frac{\Delta\bar{H}_t}{\Delta\bar{G}}=\frac{1}{F\left(s\right)-\frac{1}{2}} \tag{23}$$

3.3.3 Simplified model

Excluding the surge tank and considering in this way only the high-frequency effects of the water hammer, the following equation should be used [5]:

$$F\left(s\right)=\frac{\Delta\bar{U}_t}{\Delta\bar{H}_t}=-\frac{1}{\phi_p+Z_p\tanh\left(T_{ep}s\right)} \tag{24}$$

3.4 Experimental penstock pressure

All the quantities presented in the previous equation have been evaluated by means of available data and by experimental data. For instance, the experimental gate opening described by the servomotor position and the experimental and the simulated penstock pressure at gate are reported in Figure 9. In particular, the model of the plant including the turbine, the penstock, the surge tank and the reservoir has been tuned using the experimental gate opening reported in the upper part of Figure 9 as input of eq. (22) and evaluating the simulated penstock pressure at gate by means of eq. (23). In the lower part of Figure 9, both the experimental and the simulated penstock pressures at gate are

reported. It is possible to observe the long period oscillation of the water pressure at gate of about 225 s, due to the reservoir and the surge tank interaction, and the water hammer phenomena at time t=375 s, t=450 s and t=715 s. The water hammer phenomena at t=500 s, t=575 s and t=800 s have not been identified by the model and could be ascribed to the interaction of the water with the other elements of the systems not included in the model such as the by-pass conduit, the main spherical valve and the conduit of the second power unit.

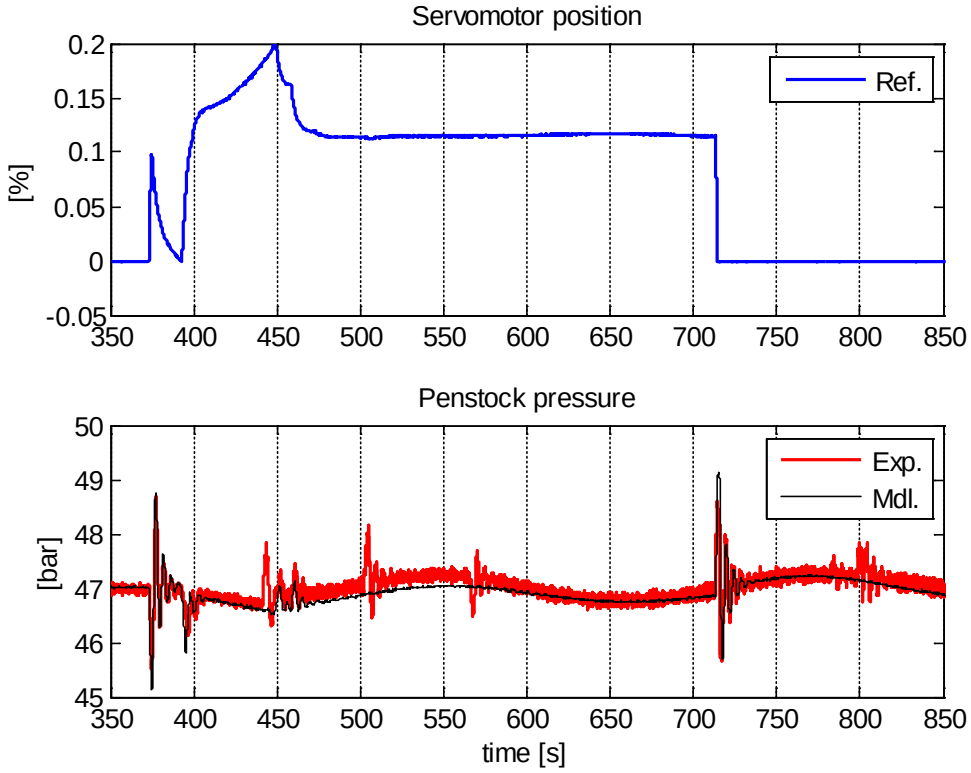

Figure 9 Experimental gate opening (upper) and simulated and experimental penstock pressure at gate (lower).

3.5 Load model

The simple torque equilibrium equation at the turbine shaft allows the insertion in the model of both the electrical load torque $\overline{T}_e$ (p.u.) and the inertia of the rotor:

$$\Delta\overline{\omega} = \frac{1}{T_a s + D}\left(\overline{T}_m - \overline{T}_e\right) \tag{25}$$

where $\overline{T}_m$ is the p.u. mechanical torque given by the turbine, D the damping factor,

$\Delta\bar{\omega}$ the p.u. rotational speed deviation and T_a the mechanical starting time. The mechanical starting time is obtained by the inertia constant $K_i = T_a/2$ that it is defined by the ratio of the kinetic energy of the rotor at rated speed ω_0 and the rated electrical power of the generator $(VA)_0$:

$$K_i = \frac{1}{2}\frac{J\omega_0^2}{(VA)_0} \tag{26}$$

Inertia J and damping D change depending on the operating conditions in the model. For instance, during a closure manoeuvre of the gate, both J and D decrease due to a reduction of the water present in the runner. The mechanical starting time T_a linearly changes in the range $8.5 \div 9\,\mathrm{s}$, whereas D in $0.06 \div 0.1$ as function of the normalized gate opening limits $0 \div 1$. In this way, the model is linearized about different steady-state operating points. A change of the damping factor also includes nonlinear variation of the turbine efficiency for different operating points [12].

Regarding the electrical load, all electrical devices such as the generator, the transformers and the power network have not been modelled in detail [13]. The experimental electrical load T_e has been used as input in the model simulations.

4 EXPERIMENTAL TESTS

As above mentioned, the considered plant is an early restoration plant and a partial revamping involved the control system of the distributor. For these reasons, the experimental data are acquired during some inspection tests of restoring procedures of the plant control system. In particular, they were aimed at verifying the proper working of the overall system and have been performed by sending suitable signals to the control system. For instance, complete closures of the main spherical valve or some disturbances on the reference speed signal have been simulated.

In particular, two different sets of tests have been carried out only on one of the two units, with the spherical valve of the second unit completely closed. The first set has regarded the correct working of the revamped control system of the servomotor, whereas the latter has been carried out on the overall system in order to test several operating conditions.

4.1 Tests on the control system of the servomotor

The tests on the revamped servomotor control system have been carried out in standstill conditions with the main valve closed and without electrical load.

The experimental data acquired during these tests have been used to tune the parameters and the time constants of the described models for the gate position controller, the servovalve and for the servomotor.

Considering the control block diagram of the gate position reported in Figure 8, the tests have been performed applying square and triangular wave reference signals as input of the outer gate position control loop G_0 or directly as current input I_0 of the servovalve in the inner loop. The experimental simulated data for reference current signals applied as input of the servovalve controller are reported in Figure 10. The position of the spool of the servovalve and the position of the stem of the hydraulic cylinder that moves the distributor are reported in the figure. In the left part of Figure 10, the reference signal of the servovalve is a full square current wave in the range of 4-20 mA with a period of 60 s. The servovalve spool reaches its physical limit of -1 to 1 mm, where the stem cylinder shows its maximum positive and negative speeds. The maximum stroke of about 135 mm of the cylinder corresponding to gate opening of $\bar{G} = 1$, is considered in the model. The reference signal of the servovalve is a triangular current wave in the range of 11.5-14.5 mA with a period of 120 s in the right part of Figure 10.

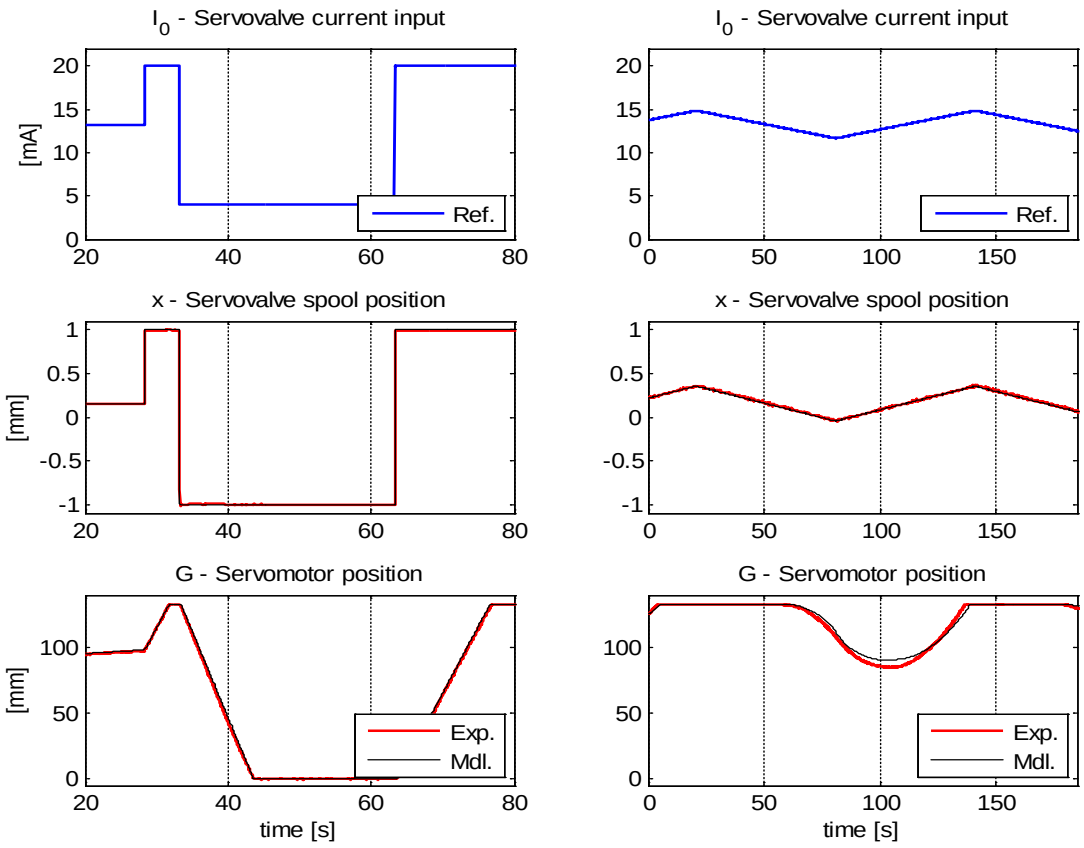

Figure 10 Tests on the inner loop of gate position control scheme: 100% square current wave (left) and triangular wave (right) reference signal as input of the servovalve.

The experimental characteristic of the servovalve, which relates the servovalve spool position x to the oil flow q_{oil} in the cylinder, as expressed by the ideal and linear relation of eq. (4), has been obtained by means of tests performed on the inner position loop of the servovalve. These results are shown in Figure 11, where it is possible to observe the nonlinearity across the middle point of the servovalve spool.

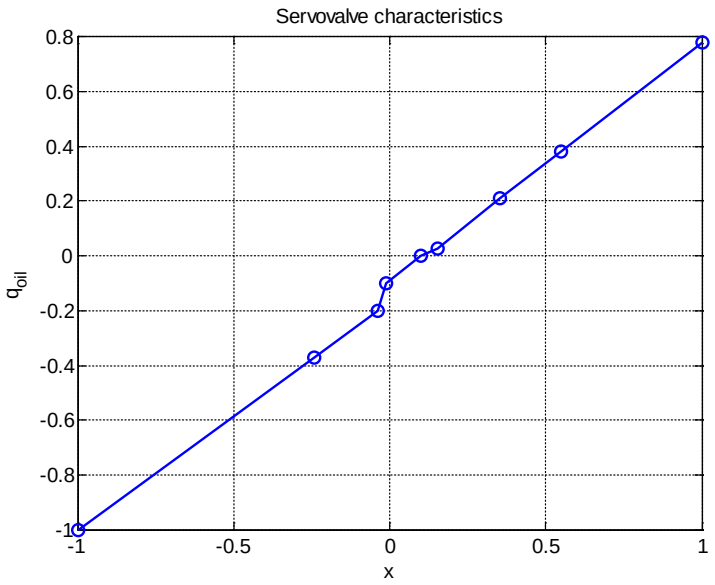

Figure 11 Characteristics curve of the servovalve obtained from experimental data.

4.2 Tests on the overall system

The second set of tests has been carried out on the overall system in order to test several operating conditions:

A) starting procedure from standstill to rated speed, idling electrical load;

B) step reference speed signals at rated speed then stop in idling electrical load;

C) full stop from rated condition (speed and load) closing both to the distributor and the spherical valve;

D) full load cut out at rated speed.

For the sake of brevity, only the first and the last interesting operation conditions are reported in the following subsections.

4.2.1 Starting from standstill to rated speed condition

The rotational speed, the gate opening and the pressure in the penstock at the spherical valve are reported in Figure 12, for the starting procedure from standstill to the rated speed in absence of the electrical load where the speed controller is the PI of eq. (1). The rotational speed reaches the rated value in about 100 s, where the model shows a negligible speed overshoot with respect to the experimental data. The rated

condition in absence of the load is reached with a partial opening of the gate (about 12%).

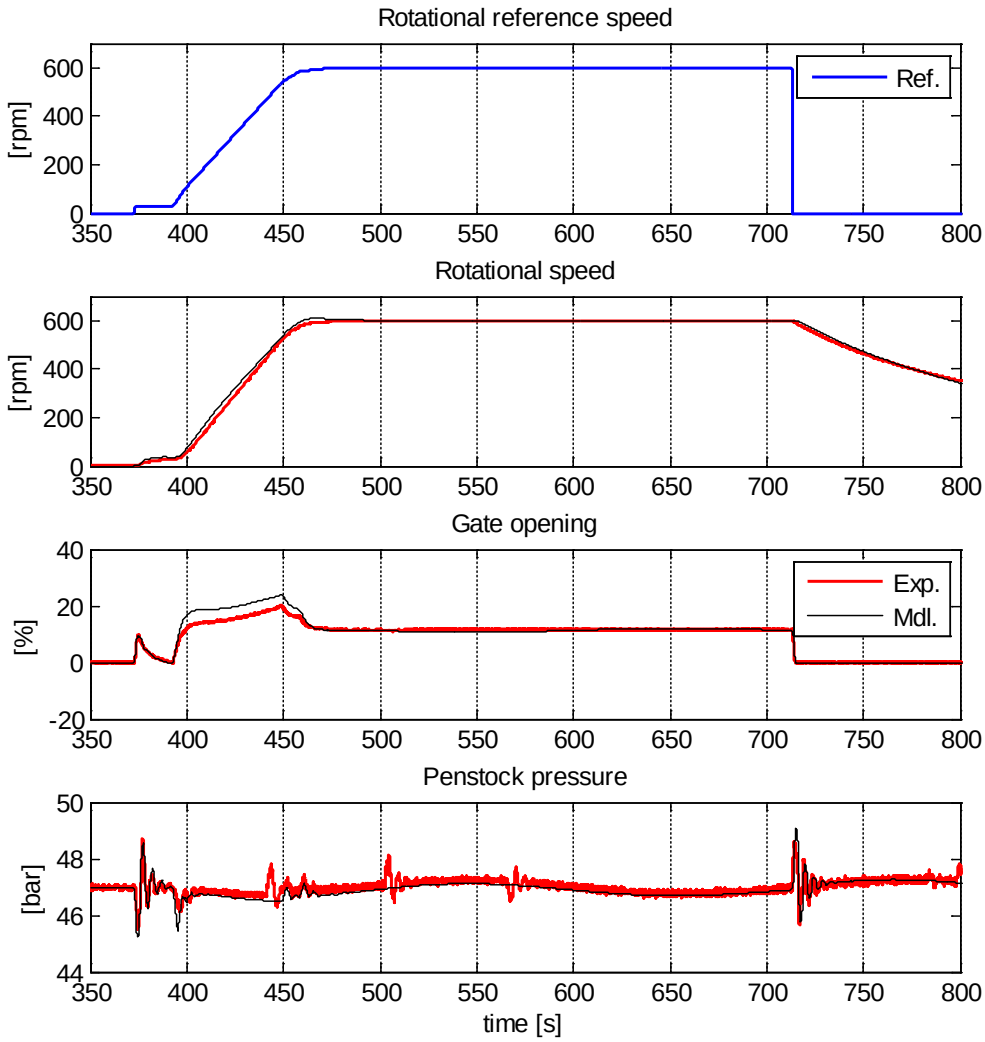

Figure 12 Rotational speed, gate opening and penstock pressure at gate for the starting test from standstill to rated speed.

An emergency condition is simulated at time 710 s, by putting to zero the reference speed signal of the speed regulator and consisting in a complete closure of the distributor in about 1.5 s; accordingly, the rotational speed decreases. As already mentioned in the previous section, some water hammer phenomena, not described by the model, occur at about time t=500 s and t=575 s.

4.2.2 Full load cut out at rated speed condition

The electrical load cut out at rated speed is analysed in this case. This condition is extremely dangerous because a turbine overspeed occurs, as shown in the upper diagram of Figure 13, where the rotational speed, the gate opening, the penstock pressure and the active electrical power are also reported. The electrical load is linearly applied starting from time t=72 s till t=95 s and is completely removed at time t=137 s as appears from the last diagram of the figure, by disconnecting the generator from the power network. The experimental overspeed is about 40% whereas the simulated one is about 50% of the rated speed. The difference between the experimental and the simulated overspeed could be ascribed to the nonlinearity of the damping of the system described by eq. (25).

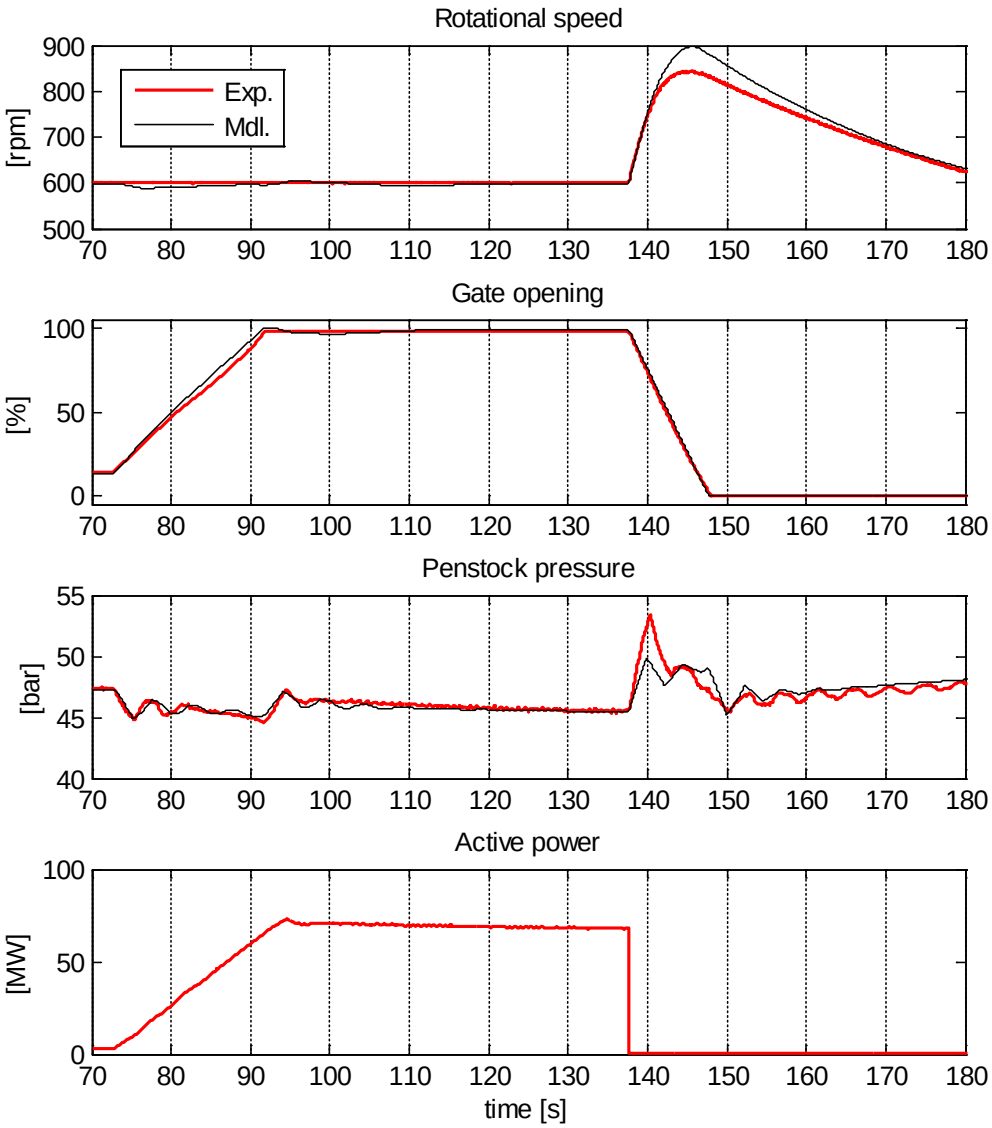

Figure 13 Rotational speed, gate opening, penstock pressure at gate and active electrical power for the load cut out at rated speed condition.

The actual and the ideal straight line speed-droop characteristics of the considered Francis turbine are shown in Figure 14.

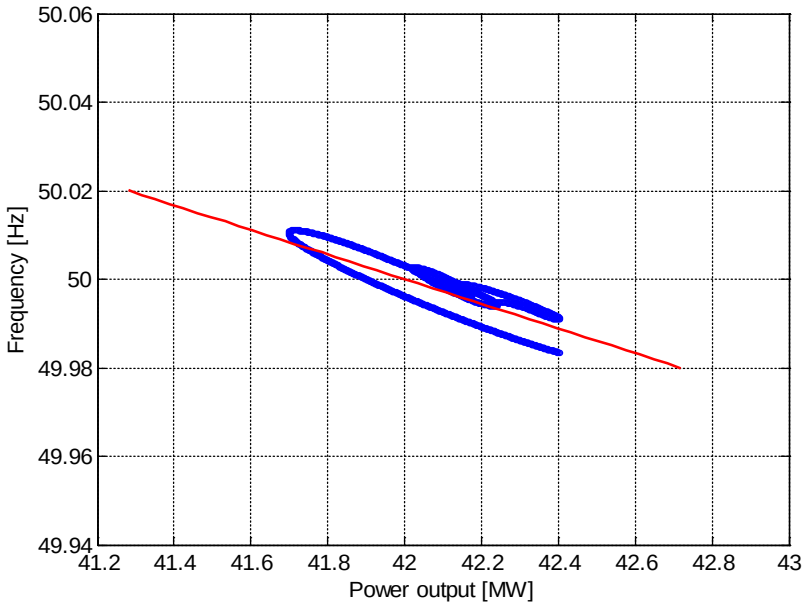

Figure 14 Actual and ideal speed-droop characteristics of the Francis turbine.

5 CONCLUSIONS

A detailed model of the overall plant of a Francis turbine hydroelectric unit has been designed and successfully tested as described in the paper.

The model is developed with the transfer function approach and includes the servovalve-servomotor control loop, the effects of the travelling waves between the reservoir and the surge tank as well as the water hammer phenomenon.

It was tuned and verified by means of experimental data acquired during some inspection tests performed after a revamping of the distributor control unit and used as reference response to validate the required test of restoring procedure of the same plant.

The model is very useful for simulating critical conditions as overspeed and water hammer phenomenon.

6 REFERENCES

[1] Byerly R.T., Aanstad O., Berry D.H., Dunlop R.D., Ewart D.N., Fox B.M., Johnson L.H., Tschappat D.W., Dynamic models for steam and hydro turbines in power system studies, *IEEE Transactions on Power Apparatus and Systems* , Vol.**PAS-92**, No.6, (1973), pp.1904-1915.

[2] Oldenburger R., Donelson Jr. J., Dynamic Response of a Hydroelectric Plant,

Transaction of the American Institute of Electrical Engineers, Vol.**81**, No.3 (1962), pp.403-418.

[3] Working Group on Prime Mover, Hydraulic turbine and turbine control models for system dynamic studies, *IEEE Transactions on Power System*, Vol.**7**, No.1 (1992), pp.167-179.

[4] De Jaeger E., Janssens N., Malfliet B., Van De Meulebroeke F., Hydro Turbine model for system dynamic studies, *IEEE Transactions on Power Systems*, Vol.**9**, No.4, (1994), pp.1709-1715.

[5] Kundur P., *Power system stability and control*, (1994), EPRI Editors.

[6] Schleif F.R., Wilbor A.B., The coordination of hydraulic turbine governors for power system operations, *IEEE Transactions on Power Apparatus and Systems*, Vol.**PAS-85**. No.7, (1965), pp.750-758.

[7] Undrill J.M., Woodward J.L., Nonlinear hydro governing model and improved calculation for determining temporary droop, *IEEE Transactions on Power Apparatus and Systems*, Vol.**PAS-86**, No.4, (1967), pp.443-453.

[8] Hannett L.N., Feltes J.W., Fardanesh B., Field tests to validate hydro turbine-governor model structure and parameters, *IEEE Transactions on Power System*, Vol.**9**, No.4, (1994), pp.1744-1751.

[9] Ramey D.G., Skooglund J.W., Detailed hydrogovernor representation for system stability studies, *IEEE Transactions on Power Apparatus and Systems*, Vol.**PAS-89**. No.1, (1970), pp.106-112.

[10] Larock B.E., Jeppson R.W., Watters G.Z., *Hydraulics of pipeline system*, CRC Press, (2000).

[11] Afshar M.H., Rohani M., Water hammer simulation by implicit method of characteristic, *International Journal of Pressure Vessels and Piping*, Vol.**85**, No.12, (2008), pp.851-859.

[12] Tzuu Bin Ng, Walker G.J., Sargison J.E., Modelling of transient behaviour in a Francis turbine power plant, *15th Australian Fluid Mechanics Conference*, (2004), pp.1-4.

[13] Okou F.A., Akhrif O., Dessaint L., A robust nonlinear multivariable controller for multimachine power systems, *Proceedings of the 2003 American Control Conference*, Vol.3, (2003), pp.2294-2299.

Figure Captions:

Figure 1 Hydraulic scheme of the first plant.

Figure 2 Spherical valve at the end of the penstock.

Figure 3 Upper part of the generator exciter system.

Figure 4 Distributor system of the Francis turbine.

Figure 5 Hydraulic control unit of the servomotor.

Figure 6 Functional block diagram of the overall system.

Figure 7 Speed controller block diagram.

Figure 8 Block diagram of the gate position control loop.

Figure 9 Experimental gate opening (upper) and simulated and experimental penstock pressure at gate (lower).

Figure 10 Tests on the inner loop of gate position control scheme: 100% square current wave (left) and triangular wave (right) reference signal as input of the servovalve.

Figure 11 Characteristics curve of the servovalve obtained from experimental data.

Figure 12 Rotational speed, gate opening and penstock pressure at gate for the starting test from standstill to rated speed.

Figure 13 Rotational speed, gate opening, penstock pressure at gate and active electrical power for the load cut out at rated speed condition.

Figure 14 Actual and ideal speed-droop characteristics of the Francis turbine.

Table Caption:

Table 1. Data of the hydroelectric central